PERFORMING GAIT PHASE DETECTION ON HEALTHY AND POST-STROKE SUBJECTS USING JOINT ANGLES DERIVED FROM IMU SENSOR DATA

RENS WASSER

UNIVERSITY OF TWENTE.

BACHELOR OF SCIENCE THESIS
Biomedical Engineering
Biomechanical Engineering
Engineering Technology
University of Twente

December 2023 – version 1.1

DOCUMENT NUMBER: BE-975

BACHELOR ASSIGNMENT COMMITTEE

Chairman:	Prof. dr. ir. Massimo Sartori
Supervisor:	Dipl.-ing. Donatella Simonetti
External member:	Dipl.-ing. Junhao Zhang Meng

CHAIR

Biomechanical Engineering

Faculty of Engineering Technology

University of Twente

Rens Wasser: *Performing gait phase detection on healthy and post-stroke subjects using joint angles derived from IMU sensor data*, Bachelor of Science thesis © December 2023

ABSTRACT

Gait analysis performed with wearable and non-wearable sensors is necessary to evaluate gait for biomechanical research, clinical rehabilitation and physical performance optimization. By utilizing a setup consisting of only IMU, a method can be actualized that is non-intrusive, has comparatively low costs and can be used outside of lab-constrained environments. This thesis presents the utilization of a novel algorithm for the detection of gait events in both healthy and post-stroke subjects, using key points in joint angles derived from IMU data. In addition, it was attempted to use data from one leg to estimate gait events from the contralateral leg. IMU and GRF data from three healthy subjects recorded at 0.9, 1.8, 2.7, and 3.6 km/h, and two post-stroke subjects recorded at a self-selected comfortable speed and their fastest walking speed were utilized for evaluation of the algorithm. Joint angles of the hip, knee, and ankle were computed utilizing Opensim. IMU-derived time points were compared with the reference data that was obtained from the GRF, and calculated in the form of offset and RMSE. Results showed that at 0.9 and 1.8 km/h, the algorithm did not perform precise and accurate enough time points to be valid. At speeds 2.7 and 3.6 km/h, the methodology showed better results, with an offset and RMSE that were often lower than 60ms. For post-stroke subjects, the algorithm did not perform up to standards for both walking speeds, due to high offset and RMSE. It was concluded that the utilized algorithm did not perform to the standards of clinical gait detection. However, it has shown that there is potential in IMU-based setups that utilize joint angles for gait phase detection.

ACKNOWLEDGMENTS

I would like to express my deep gratitude and appreciation to all those who have supported and guided me throughout this journey of completing my thesis. Without their assistance, this work would not have been possible.

First and foremost, I would like to thank my supervisor, Donatella Simonetti, for her patience, expertise and feedback. I appreciate her continuous support throughout this thesis. I would like to thank my family for their encouragement and understanding during this challenging process. Their belief in me has been a constant source of motivation. Lastly, I would like to thank the the members of my thesis committee, Massimo Sartori and Junhao Zhang for their valuable feedback.

CONTENTS

LIST OF FIGURES

LIST OF TABLES

ACRONYMS

HS Heel Strike
FF Foot Flat
MSt Midstance
HO Heel-off

TO	Toe-off
MSw	Mid-swing
LSTM	Long short-term memory
GRF	Ground Reaction Force
IMU	Inertial Measurement Unit
IK	Inverse Kinematics
RMSE	Root Mean Square Error

1 INTRODUCTION

Human gait, the intricate repeating pattern of movement while walking, has been intriguing researchers for a long time due to its importance for assessing health and physical performance. The evaluation of the human gait is called gait analysis and has significance in multiple fields, including biomechanical research[1] clinical rehabilitation[2] and physical performance optimization[3]. In the context of clinical applications, performing gait analysis is crucial for devising targeted interventions to address gait-related abnormalities[4], to measure the efficacy of rehabilitation[5], to monitor and diagnose diverse musculoskeletal and neurological diseases such as Parkinson, multiple sclerosis and stroke[5, 6]. The methodologies used for gait analysis have evolved from subjective visual assessment to instrument-assisted methodologies. For subjective visual assessment, subjects were often filmed and footage was reviewed based on scoring systems. Points were given to observed gait scales such as gait parameters, body segment positions or performance on timed tasks[7]. The main advantages are the speed to evaluate major abnormalities and the method being non-obtrusive and inexpensive due to the absence of measurement devices. However, the method is relatively subjective in nature and it may lead to poor validity, reliability, sensitivity, and specificity compared to instrumented gait analysis[8]. The current technological devices that are used to perform gait analysis can be classified into two approaches: non-wearable sensors and wearable sensors. Non-wearable sensors can be further classified into methodologies that use force platforms or pressure measurement systems as floor sensors and those using camera-based tracking systems that utilize motion capture with or without markers. Floor sensors are used to measure ground reaction forces or quantify pressure patterns, while camera-based tracking systems are used to obtain joint kinematics and kinetics, and establish a three-dimensional motion analysis. The methodology for wearable sensors uses different types of sensors located on the body, including accelerometers, gyroscopes, magnetometers, force sensors and electromyography. These sensors are used to measure various data to characterize human gait such as acceleration, angular velocity, sensor orientation, ground reaction forces and relative muscle tension[5].

The data from the wearable and non-wearable sensors can be correlated to each gait phase by utilizing the biomechanical characteristics of each phase. Ground reaction forces can be utilized to obtain certain gait parameters, such as gait cycle duration, frequency and symmetry, due to the start and end of the measured force in each gait cycle. The kinematic and kinetic data can be utilized for movement modeling and calculating changes in joint angles, moments or velocity. The change of velocity of body segments, such as the shank or foot, or certain positions of joint angles can be used to determine gait events. Gait events indicate the start and end of gait subphases and are crucial for gait analysis.

Despite the advancements in gait analysis, accurate gait phase detection remains a challenging process in clinical applications. The gold standard for gate phase detection often involves advanced setups bound to a laboratory, consisting of a multi-camera motion capture system in combination with force plates [9]. This gold standard setup provides the best accuracy and information on related gait dynamics. However, the employment of such setups is quite limited due to their costs, the time constraints, the intrusiveness of equipment, and the lab-constrained

environment. Contrary, Inertial Measurement Units Inertial Measurement Unit (IMU)s offer the advantage of non-intrusiveness, comparatively low costs and usage in a non-restricted working environment. Thereby creating a possible solution for gait phase detection outside of lab-constrained working environments such as private clinics.

However, there are a few challenges with employing IMUs instead of utilizing the gold standard setup for gait phase detection. First of all, comparable accuracy needs to be achieved while utilizing a lesser quantity of sensors. In addition, IMUs have the disadvantage of introducing inherent noise and errors, due to factors such as signal drift, inconsistent sensor placement and synchronization[10]. These challenges can mostly be solved by strict setup methodology and using filters during data processing. Furthermore, the use of IMUs limits the complexity of the setup by reducing setup duration and inconsistencies in sensor placement.

Research on gait phase detection utilizing only IMUs has already been conducted with various methodologies. In the study of Soliman et al.[11] the angular velocity of the shank was utilized to obtain initial and final contact by correlating them to peaks in the angular velocity. Due to its sample size, the study was limited in its usage on people with neurological or major physical impairments. In addition, by only using one IMU the study was only able to measure kinematic data for one segment of the body, limiting further expansion by utilizing f.e. joint angles. A study by Lora-Millan et al.[12] utilized four IMUs on the pelvis, right thigh, shank and foot with an extended Kalman filter to obtain joint angles. Gait events were correlated to maxima, minima and distinct angles. The methodology was only limited by the requirement of a rich enough movement around the sagittal axis to fulfill the one-axis restriction in the knee joint. In addition, the methodology was not utilized on data sets from impaired subjects. All these methods are explained in more detail in section 2.3

The main aim of this bachelor thesis is to develop an IMU-based strategy for gait phase detection, by utilizing a strategy that uses key points in joint angles. Furthermore, there are two additional aims:

- An additional aim is to see if the methodology can be utilized on both healthy and post-stroke subjects
- In addition, gait event estimations on the non-recorded contralateral leg will be performed with the data of the recorded leg. To determine if it is possible to use data from the recorded leg to obtain gait event data for both legs.

This thesis is structured as follows: chapter 2 will provide an overview of existing literature on gait analysis and gait phase detection techniques with IMUs. chapter 3 discusses the adopted methodology, including data collection, sensor configuration, and data processing algorithms. chapter 4 presents the results, showcasing the effectiveness of the proposed strategy. In chapter 5, a discussion of the results can be found with limitations of the proposed methodology and recommendations for future research. Lastly, chapter 6 provides a summary of the thesis's findings.

2

THEORY

This chapter describes the fundamental theory of human gait, IMU gait phase detection and the utilized software to process data.

2.1 HUMAN GAIT

Human gait consists of a repeating cyclic pattern divided into two main phases, stance and swing phase. These phases can be further classified into sub-phases, which are bordered by gait events, as can be seen in figure 1. The stance phase, *i.e.*, the part of the gait cycle where the foot contacts the surface while bearing body weight, occupies around 60% of the gait cycle. It can be classified into five sub-phases: the heel strike, loading response, midstance, terminal stance and the preswing. These sub-phases correspondingly start from the following gait events: Heel Strike (HS), Foot Flat (FF), Midstance (MSt), Heel-off (HO) and Toe-off (TO). The swing phase is the part of the gait cycle where the foot has no contact with the surface, in other words, the period between TO and HS. It can be classified into three sub-phases: the initial swing, Mid-swing (MSw) and the late swing[13, 14].

Each gait phase is characterized by well-defined biomechanical features. Information on the dictating gait events and changes in joint angles of each sub-phase is explained in the following list[13, 14]:

1. Initial contact

   The gait cycle starts with the stance phase, initiating a double limb support by initial contact with the right leg. The corresponding gait event is the HS. The knee is in a stable, fully extended position while the ankle is dorsiflexed. The hip slowly extends from full flexion, starting the transition to the loading response.

2. Loading response

   The loading response starts at FF, where the foot is fully planted on the support area. The knee starts a slight flexion wave that dips to 15-20° after which it extends. The ankle creates further forward propulsion by plantar flexion and the hip slowly moves into extension. At the end of FF, the body is fully supported on one leg and while moving forward, transitions towards midstance.

3. Midstance

   When the greater trochanter of the femur is directly above the middle foot, the body is at MSt and starts the midstance sub-phase. The knee is fully extended, ending the flexion wave. The ankle supinates and dorsiflexes, and the hip moves from flexion to extension.

4. Terminal stance

   After MSt, the gait transitions into the terminal stance at HO, which is the moment when the heel leaves the surface. The full bodyweight will be focused on the metatarsal heads of the foot. The knee flexes slightly, the ankle supinates and plantar flexes, and the hip first hyperextends, to then go into flexion.

5. Preswing

   At the end of the terminal stance, the contralateral leg will start initial contact by HS, once again initiating double limb support. While the body moves forward, it pushes off the surface and goes into the preswing at TO, where the knee flexes to 35-40°, the ankle further plantar flexes and the hip is less extended. During TO the toes are pushed into the ground creating a burst of forward propulsion, ending surface contact and entering the swing phase.

6. Initial swing

   In the initial swing the knee flexes to 40-60°, the ankle starts dorsiflexing until it is in a neutral position and the hip transitions from extension to flexion while laterally rotating.

7. Mid-swing

   The mid-swing starts at the MSw event, which is where the foot passes the contralateral foot. The knee flexes to 60° and then quickly extends by approximately 30°. The ankle dorsiflexes and the hip will have maximum flexion.

8. Terminal swing

   After the mid-swing, the gait cycle enters the terminal swing, where the leg is preparing to reestablish double limb support and restart the gait cycle. The knee goes to full extension, the ankle moves gradually to a neutral position towards the end of the terminal swing and the hip has a slight extension. The terminal swing is the end of the swing phase and the gait cycle. It transitions into initial contact, starting the stance phase and restarting a new gait cycle.

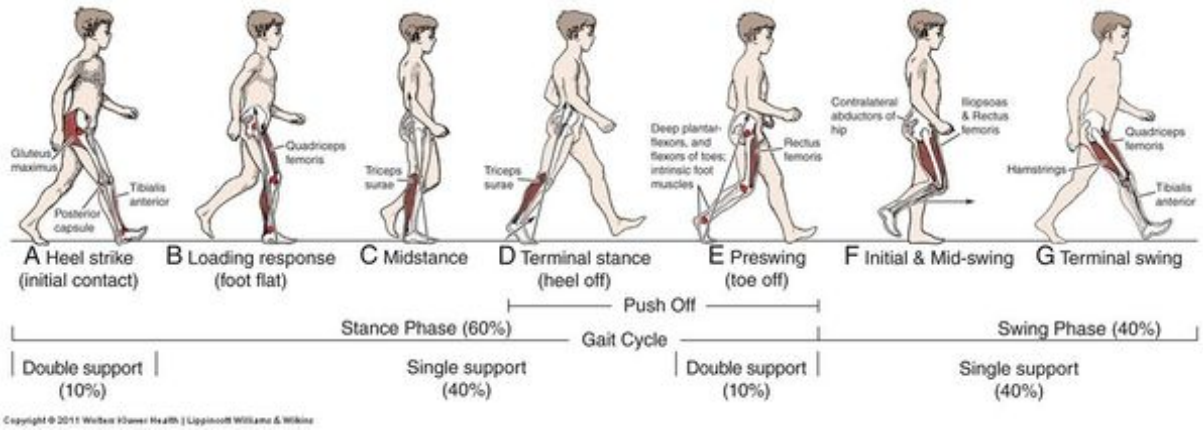

Figure 1: Illustration showing the gait cycle phases and its stances, including double and single leg support stances[15]

2.2 INERTIAL MEASUREMENT UNITS

Inertial Measurement Units have proved to be very useful in biomechanics and motion analysis due to their compact size, portability, and comparatively low cost. A typical IMU always consists of at least two sensors, a 3-axis accelerometer and 3-axis gyroscope, and sometimes has a third sensor, a 3-axis magnetometer. These sensors establish either a six or nine degrees

of freedom IMU that can measure specific aspects of an object's motion, providing valuable data for gait and motion analysis. This section provides an overview of the key components and principles of IMUs[16].

Accelerometers are designed to measure linear acceleration. They operate based on the fundamental principle of Newton's second law, which states that the force acting on an object is directly proportional to the rate of change of its linear velocity. Within an accelerometer, there is a proof mass that gets displaced by an exertion of force due to acceleration. This displacement can be detected by a pick-off and is converted into an electrical signal, which can be scaled to indicate acceleration. The sensor's output is typically expressed in units of gravity (g), where 1 g represents the acceleration due to gravity. By integrating the accelerometer's output over time, the velocity and thus the displacement information can be obtained[16, 17].

Gyroscopes are sensors that measure angular rates for an inertial frame of reference. Gyroscopes utilize the principle of angular momentum conservation. When an angular acceleration is applied, a torque is exerted on the gyroscope, which causes its precess around an orthogonal axis. The gyroscope's output is proportional to the rate of this precession and can be used to calculate angular rates. By integrating the angular rates over time, the change in angle concerning an initial reference angle can be obtained. The change in angle can be further utilized to determine the angular position or orientation of an object[16, 17].

As said before, some IMUs are equipped with magnetometers, which are sensors that measure the strength and direction of a magnetic field. These sensors are mainly utilized for applications where knowledge of the device's orientation relative to the Earth's magnetic field is essential. In gait analysis, they can be used to determine the orientation of the IMU to the Earth's magnetic north, providing additional information about the sensor's spatial orientation. When combined with the data from the accelerometer and the gyroscope, an absolute heading can be determined[16, 17].

One of the key challenges of IMUs is the need for precise calibration and sensor fusion. Due to inherent sensor biases, scale factor and other systematic errors, IMU data can drift over time, leading to inaccuracies in its motion estimation. To minimize these issues, calibration procedures are essential. This involves characterizing and correcting sensor errors to ensure the accuracy and reliability of the IMU measurements[16, 17].

Sensor fusion is another critical aspect that combines data from the sensors within the IMU. Sensor fusion algorithms, such as complementary filters or Kalman filters, integrate data from multiple sensors to provide a more accurate estimate of motion and orientation. In addition, sensor fusion can be utilized as a method to eliminate errors from sensors. For example, if the gyroscope has a small, consistent angular rate, but the magnetometer and accelerometer show no sign of motion. Then it can be inferred that the gyroscope is giving a false output that needs to be adjusted[16, 17].

2.3 INERTIAL MEASUREMENT UNITS FOR GAIT PHASE DETECTION

There are multiple methods to establish gait phase detection, including image processing, force sensors and wearable sensors[5]. Where an image processing method utilizing optoelectronic systems is generally considered the gold standard, due to their high accuracy in kinematic feature measurements[9]. However, this thesis will focus on a strategy that deviates

from the gold standard by only utilizing wearable IMU sensors.

Most research that involves gait phase detection by IMUs focuses on two phases, whereas most publications mainly focus on the separation between stance and swing, indicated by the heel strike and toe-off. These studies contain several methods that often utilize either one or two IMUs to obtain events for one side. One of these methods is based on angular rate measurements. An example is Sarshar et al.[18], which is a proof of concept where raw data was obtained by an IMU at the shank and processed to a smoothed angular velocity magnitude. This data was then put through three Long short-term memory (LSTM) algorithms that extracted HS, MSt and TO events as data comprising the probability in a time series. It concluded that LSTM models could be used to predict gait phases, however, the LSTM model might need to be retrained and improved for better results. While this study shows that HS, MSt and TO can be detected with the angular rate of the shank, the applied algorithm was too complex to replicate. Another study from Soliman et al.[11] utilized an IMU setup similar to Sarshar et al.[18] to detect initial and final contact in straight-line walking. The initial and final contacts were related to the negative peaks in the mediolateral angular velocity. This showed that the events of HS and TO could be predicted by detecting certain points in the mediolateral angular velocity of the shank. This would be one of the methodologies that could detect the most important gait events and parameters with the least amount of IMUs, however, obtaining gait event outside of HS, MSt and TO would be quite hard with angular velocity data. Not only due to missing key points but also having significant noise artifacts.

Another method that is utilized is based on joint angles obtained from combining the IMU kinematic data with Inverse Kinematics (IK). For instance, the study by Park et al.[19] used seven IMUs placed on the pelvis and for both legs on the frontal distal thigh, frontal medial shank and upper foot. For the reference, they used a motion capture system. The study concluded that the hip-joint angle during walking showed no significant difference ($p > 0.05$), while the knee and ankle joints did show significant differences in certain variables ($p < 0.05$). However, the differences were in maximum, minimum and range of motion variables. All three joints showed decent comparability along the gait phase in terms of local maxima or minima. While this study is more focused on comparing joint angles, it is a good foundation to be utilized in gait phase detection, seeing as the joint angles along the gait phase were adequately comparable. This could potentially open up the possibility to utilize key points in the joint angles for gait events, as done with the angular velocity in the study of Soliman et al. One more study that is based on joint angles is Lora-Millan et al.[12] evaluated an Extended Kalman Filter for gait detection with sagittal lower limb kinematics. The filter that was utilized to conduct the evaluation was established in earlier original work and adapted for their more recent study.[20] They performed the study with four IMUs, strapped to the pelvis, right thigh, right shank and right foot. For gait event detection, certain maxima, minima and distinct angles were noted as key points. For example, a maximum angle for the knee indicated an early stance and a maximum angle from the hip indicated a mid-stance. This study shows that joint angles from the hip, knee and ankle could be utilized to identify the six gait events from the IMU applied to the leg. The study concluded that the algorithm could be utilized as a controller for wearable robotic devices. However, while they applied their methodology on eight healthy subjects, they did not test the algorithm on impaired subjects. In addition, the study only evaluated the gait events from the right leg, without looking at bipedal events. There might be a possibility to also evaluate the left leg with certain key points from the right leg.

2.4 MOVEMENT MODELLING

To simulate movement and obtain joint angles, an open-source software program called OpenSim was utilized.[21]
To be able to utilize this program, a model needs to be constructed, which involves a codified description of the topology and dynamics of a biomechanical system. This can not only include skeletal, neural and muscular structures, but also components of non-biological nature, such as exoskeletons. This can be done manually by defining the components such as rigid bodies and muscles, that will prompt OpenSim to generate a system that includes equations that control the kinematics and dynamics of that constructed model. These computations are done by the program Simbody, using an order-N recursive formulation. Simbody is one of the various tools that OpenSim utilizes to operate. If one does not have all the necessary data to construct a model, a generic model provided by OpenSim to simulate data can be chosen[22].

To get a more accurate simulated subject, the model can be scaled in OpenSim[23]. This can either be done by measurement-based or manual scaling. For measurement-based scaling, a file containing all markers on the model and experimental marker positions needs to be provided. By comparing the distance between the experimental and virtual marker positions, scale factors are created for individual segments. These individual factors can also be combined into an overall scale factor, which can be used to generally scale all segments. Manual scaling provides the possibility to scale any individual segment manually. The scale factors can be determined by manually measuring the length of segments of a subject, which has a higher precision than scaling the full model by the difference in height between a generic model and the subject. Based on these provided scale factors, an algorithm will scale all body frames and their related objects, such as joint frame locations and muscle attachment points. In addition, by inputting the body mass of the simulated subject, the body mass of the model can be scaled proportionally, by scaling factors and thus changing the body mass of the model or by scaling factors while body mass stays preserved.

2.5 INVERSE KINEMATICS

Inverse Kinematics IK is a mathematical approach used to determine the joint angles and positions of a kinematic chain given the desired end-effector position and orientation. For motion analysis of gait with OpenSim, IK can be performed either using IMU or marker data to estimate joint angles and positions of body segments.

Applying IK on IMU data first requires the use of the IMU placer tool, which places virtual IMUs onto the model by utilizing quaternion data,i.e., IMU sensor orientation, of a calibration motion file. Once each IMU is registered to a specific body segment, the IMUIK tool can be used to simulate experimental movement by computing coordination values for each time frame of motion. The coordination values position the model in a pose that best reflects the experimental IMU orientation. In a mathematical context, the 'best match' is expressed by the weighted least squares problem. The solution to this problem aims to minimize orientation

errors and is computed by the IMUIK tool[24]. The solution provided by the IMU IK tool can be defined as:

$$Weighted\ Least\ Squares\ Equation = \min_{q} \sum_{i=IMUs} w_i {\theta_i}^2 \tag{1}$$

Where q is the vector of the generalized coordinates, w_i is the weights corresponding to each IMU orientation, and θ_i is the angle component of the orientation errors expressed by an axis-angle representation.

3

METHODS

This chapter will describe the methods that were utilized for data collection, data processing, and results interpretation.

3.1 HUMAN GAIT DATA COLLECTION

The data that was utilized for this thesis was recorded in the Biomechanical Engineering lab in the Horst-complex at the University of Twente. In total, data for three healthy subjects (subject 1-3) were obtained during the research of Wang et al.[25] and data of two post-stroke subjects (subject 4-5) were obtained during the research of Simonetti et al.[26] with participant information for body mass, height, age and gender that can be seen in table 1. Post-stroke subjects data was only available in the form of average data across all subjects.

Table 1: Participant information of body mass, height, age and gender of subjects

Subject	body mass(kg)	height(m)	age(years)	gender
1	75.2	1.80	23	M
2	65.1	1.71	23	F
3	56	1.68	23	F
4-5	88.9 ± 16.5	179 ± 5.1	57 ± 8.7	

3.1.1 *Protocol for healthy subjects*

An experimental setup including eight IMUs and a split-belt instrumented treadmill was utilized. Eight IMUs (Xsens Link, Enschede, The Netherlands) recording at a frequency of 240 Hz, were used to measure the kinematics of the lower limbs and trunk. They were placed with straps on the sternum, pelvis, lateral side of the thighs, frontal side of the shanks, and the dorsal side of the feet. In addition, 33 reflective markers were placed on the lower limbs and trunk of the subjects. A split-belt instrumented treadmill (Motek-Forcelink BV, Culemborg, The Netherlands) was used to acquire the GRF data of the individual legs at 100 Hz.

A synchronization protocol was established that started and stopped measurements for the experiments, which can be found in Wang et al.[25]. This protocol caused the recording of data of all sensors to start and stop at the same time. First, a measurement was made where the subject stood on the treadmill and performed a 10 s standing trial for later calibration. After that, subjects were instructed to perform six walking trials (0.9, 1.8, 2.7 and 3.6 km/h) on the treadmill for around 60 seconds and each walking speed was recorded once.

3.1.2 *Protocol for post-stroke subjects*

The experimental setup included eight IMUs (Xsens Link, Enschede, The Netherlands) recording at a frequency of 100 Hz were used and placed on the pelvis, lateral side of the thighs, frontal side of the shanks and the dorsal side of the feet. Two force plates were used for acquiring the GRF data at a frequency of 1000 Hz.

First, a measurement was made where the subject performed a static standing pose in a neutral position for ten seconds for later calibration. After, all subjects were recorded while walking at a self-selected comfortable speed and their fastest walking speed. A minimum of ten gait cycles were recorded across all measurement systems for each walking speed.

3.2 ACQUISITION OF JOINT ANGLES

The data from the IMUs recorded with the Xsens software included velocities, accelerations, gyroscopic data, magnetometer data, and quaternions. Afterward, OpenSim was utilized for computing joint angles from IMU sensors orientation, *i.e.*, quaternions. Using MATLAB, the quaternions were converted into motion files for the OpenSim software. For the musculoskeletal model, the generic model gait2392_simbody was used for all subjects. This is a generic model provided by OpenSim that is primarily used for lower extremity analysis.

3.2.1 *Scaling*

Establishing a model for every subject that compared the most with their real anthropometry was done by utilizing the 'Scale Model' tool in OpenSim. Each model started with the gait2392_model which is about 1.68 m tall and has a body mass of 75.16 kg. This model was scaled for all subjects according to the following steps:

1. Changing the body mass of the model with that of the subject
2. Selecting 'Preserve mass distribution during scale'
3. Deselecting 'Adjust Model Markers'
4. Changing all scales in 'Scale Factors' by the factor $\frac{\text{Height}_{\text{subject}}}{1.8}$

3.2.2 *IMUs inverse kinematics*

First, the IMUs needed to be placed on the model, for which the 'IMU placer' tool was used. This tool took a data transformation of space-fixed Euler angles from the IMU coordinate space to the OpenSim coordinate space as input. After placing the IMUs without any rotations and the OpenSim frame having the x-axis toward the front, the y-axis upwards and the z-axis toward the left, all IMUs needed to be rotated around the X-axis by $-90°$ to obtain a representative placement of the IMU. The next input was an orientation file during the standing pose of which the first frame of quaternions is used to calibrate the initial positions and orientations of the IMUs on the pelvis, right tibia, femur and calcaneus. To obtain a correct singular frame for the static pose, the mean was taken of all frames of quaternions recorded during the static

data recordings. This singular mean frame was then converted to the orientation file and utilized.

After the IMUs were placed, the 'IMU Inverse Kinematics' tool was used to produce motion files containing joint angle data. This tool has two inputs, data transformation and sensors orientation file. For the data transformation, a rotation around the X-axis by −90° was needed. The sensor orientation file was the motion file of the desired walking speed. IMU IK was repeated for all walking speeds and for all subjects.

3.3 GAIT EVENT DETECTION

3.3.1 *Ground reaction forces*

The ground reaction forces were used as a reference for the gait events. The raw data was first filtered with a low-pass Butterworth filter to reduce noise. The data acquired at 100 Hz was filtered with a 4-th order filter and a cut-off frequency of 5 Hz. Parameters were chosen based on filters used in other articles with similar sampling frequency and comparing filter results in the range of 2-10 Hz[27, 28].The raw data acquired at 2048 Hz was filtered with a 6-th order and a cut-off frequency of 25 HZ. The high sampling rate increased the amplitude and frequency of the noise causing the need for a higher-order filter to be able to attenuate the data more aggressively and remove higher-frequency noise, a higher cut-off frequency was chosen to minimize the amount of lost information. Filter results with cut-off frequency in the range of 10-50 Hz were tested for optimal results.

Six gait events were automatically extracted for both legs. TO, HS and MSt were acquired by using the unfiltered data of the GRF and utilizing the MATLAB R2021b islocalmin command with the flatselection option. For each leg the first flat point of each cycle correlated with the TO, the center point with the MSw and the last point with the HS. For the last point, a minimum prominence needed to be utilized due to false positives in the non-zero data. Using the filtered data, the remaining FF, MSt and HO time data were obtained by utilizing the MATLAB findpeaks command. The first and second maxima, with a minimum peak height of 50% of maximum peak height to minimize false positives, indicated respectively the FF and HO. The minima with a minimum peak height of 50% of maximum peak height indicated the MSt.

For extra prevention of false positives, a minimum separation distance between peaks was used for MSt that was based on the mean distance between MSw. In addition, using MSw as reference points, every stance phase was verified for two maximum peaks and one minimum peak. If the amount of data points differed from expectations (two maxima, one minimum) all data points between the twoMSw data points were returned as false results.

3.3.2 *IMU-based strategy*

The joint angles from the IMU data were first filtered with a low-pass Butterworth filter to reduce noise. The data acquired at 100 Hz was filtered with a 3-th order filter and a cut-off frequency of 5 Hz. The raw data acquired at 240 Hz was filtered with a 4-th-order filter and a cut-off frequency of 2 Hz. Parameters were chosen due to the need for a smooth signal that contained as little noise as possible to keep false positives at a minimum. For the higher sampling rate data, a higher order with a lower cut-off frequency showed to be optimal in

comparison to a filter with equal order and higher cut-off frequency.

Key points in the hip and knee extension/flexion, and ankle plantar-dorsi flexion were defined and correlated to six gait events. as seen in table 2 and fig. 2. In addition, based on the phenomenon of reciprocal leg movement, it was assumed that when the right leg is at a certain gait event, the contra-lateral leg will be in a gait event that is half of a gait cycle further. For example, when the right leg is at the HS gait event, the left leg is assumed to be at the HO event, three gait events further. With this assumption, it was possible to estimate gait events for both legs while only utilizing IMU on one leg.

Joint	Key point	Gait event
knee	First extension maxima	HS R/HO L
	Second flexion minima	FF R/TO L
	Second extension maxima	MST R/ MSW L
	Minimum flexion	TO R/FF L TO R/FF L
hip	Minimum flexion	MSW R/MST L
	Maximum flexion	HO R/HS L

Table 2: Key point definitions that correlate with gait events. Where R stands for the gait event for the right leg and L for the gait event for the left leg.

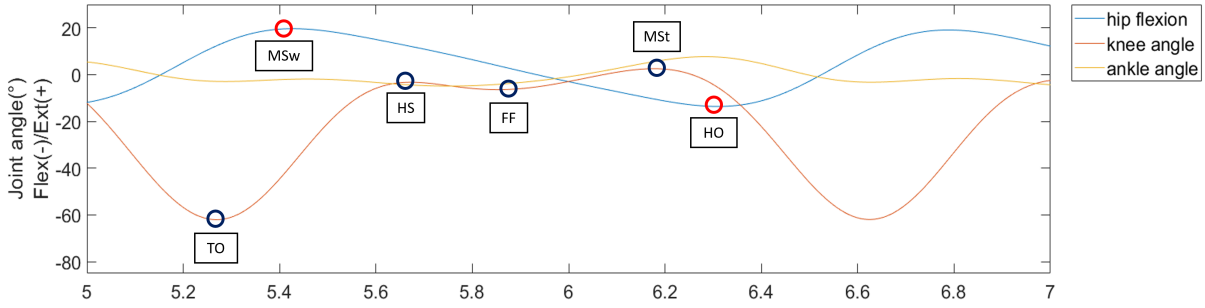

Figure 2: Graph of one gait cycle with hip, knee and ankle joint angles with points on the joint angles to visualize key point allocations. Where the red circles indicate the key points of the hip joint angle, and the blue circles indicate the key points of the knee joint angle.

An automated Matlab script based on the functions localmin and localmax gave the time of the six key points. To reduce false positives and false negatives a similar method is utilized as described in section 3.3.1. The minimum knee flexion is used as a reference point, as this was a reliable joint angle dip caused by the TO gait event, occurring right before gait initiation. The amount of maxima and minima between each n and n+1 knee joint angle dip is calculated for the knee and hip joint angles. If the amount of data points differed from expectations (two maxima, one minimum and one maximum, one minimum) all data points between the two knee joint angle dip data points were returned as false positives and indices were adjusted to prevent an impact on further processing.

In addition, to prevent false positives and negatives due to startup variation, the algorithm started at the maxima of the hip joint angle at the first gait cycle. The algorithm deleted all data points for all gait events that start at an earlier data point than the first hip joint maximum.

3.4 PRE-PROCESSING GAIT EVENT DETECTION

To be able to verify the results of the GRF and the IMU-based gait detection, they needed to have an equal amount of data points that also correlate with each other over the full gait measurement. Otherwise, the false positives will cause problems. First, the start of data collection needs to be streamlined, so both GRF and IMU data need to start at the same gait event. This required a data point that always has a high prominence and accuracy, to obtain a consistent data point. For both cases, this was the maxima of the hip joint angle. So all data points for both GRF and IMU data before the first maximum hip joint angle were deleted. In addition to a starting point, there was also an endpoint that needed to be established, because the data measurement did not consistently stop at certain time intervals. To accommodate as much data for each measurement, an array was created that contained the length of all IMU gait event data indices. Then the minimum value of the array was taken, which became the new maximum number of indices used for both GRF and IMU-based gait events.

3.5 ASSESMENT OF GAIT EVENT DETECTION

For assessment of the gait events extracted using GRF and IMU data, the mean offset with the standard deviation, the Root Mean Square Error (RMSE), and the false positives and false negatives were used. To show the accuracy of the utilized strategy, the mean offset with standard deviation was acquired by subtracting time data points of the GRF from the IMU time data points and applying a MATLAB standard deviation function on all acquired offsets. To show the precision of the utilized strategy, the false positives and negatives were acquired by verifying if the amount of measured data points was higher or lower than the expected amount. If the amount of data points was lower than expected, there was a false negative, if the amount of data points was higher than expected, there was a false positive. The RMSE was calculated with the MATLAB function rmse, where a value of 0 indicates a perfect fit with the GRF reference data, this value can be defined by the following equation:

$$\mathrm{RMSE} = \sqrt{\frac{\sum_{i=1}^{n} t_i^{GRF} - t_i^{IMU^2}}{n}}. \tag{2}$$

In this equation n stands for the total number of data points, i is a certain data point, t_i^{GRF} is data point number i from the GRF data and t_i^{IMU} is data point number i from the IMU data.

RESULTS

This chapter shows results obtained from processing the IMU data and the assessment of the methodology used for gait phase detection described in chapter 3.

4.1 JOINT ANGLES FROM IMU INVERSE KINEMATICS

In fig. 3 the results are shown from the IMU inverse kinematics for a healthy subject. It shows the knee, ankle, and hip joint angles at various walking speeds. Notable is that the basic outline of the hip stays consistent, while the knee and ankle joints both lost the amplitude hence showing smaller peaks at the slowest speed. In addition, an overall improvement in standard deviation can be observed with the increase in walking speed, suggesting that gait cycles became more consistent at higher walking speeds.

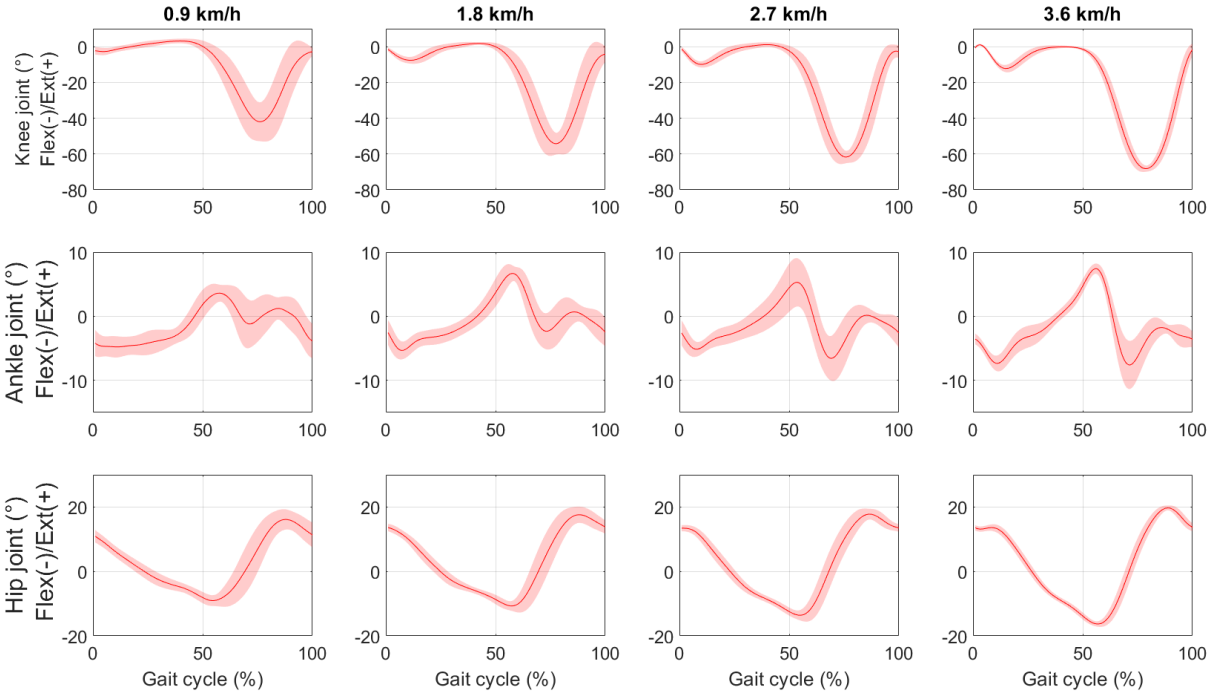

Figure 3: Joint angle results from IMU inverse kinematics from a healthy subject. Red lines show the mean angle across all gait cycles for each walking speed and joint, while the shaded area represents the standard deviation. From left to right are shown walking speeds of 0.9, 1.8, 2.7, 3.6 km/h. From top to bottom are shown knee, ankle, and hip flexion angles

4.2 COMPARISON OF REFERENCE GAIT EVENTS TO JOINT ANGLE KEY POINTS

A comparison of gait event time points obtained from the reference GRF data to the joint angles is shown in fig. 4. This figure shows the overlap due to bipedal movement between the gait events of the right and left legs. It is noticeable that the combination of FF and TO was the only combination that had a larger time discrepancy with reference data. In addition, the figure shows an overlap with the defined key points. As seen table 2 in the method section. Looking

at the figure for the joint angles, a large offset can already be seen between the key points extracted from IMU IK and the reference method. Especially for the MSt R/MSw L lines in black and brown and the HO R/HS L lines in pink and purple. These events correspond, respectively, with the key points defined as the small flexion wave and the second extension of the knee.

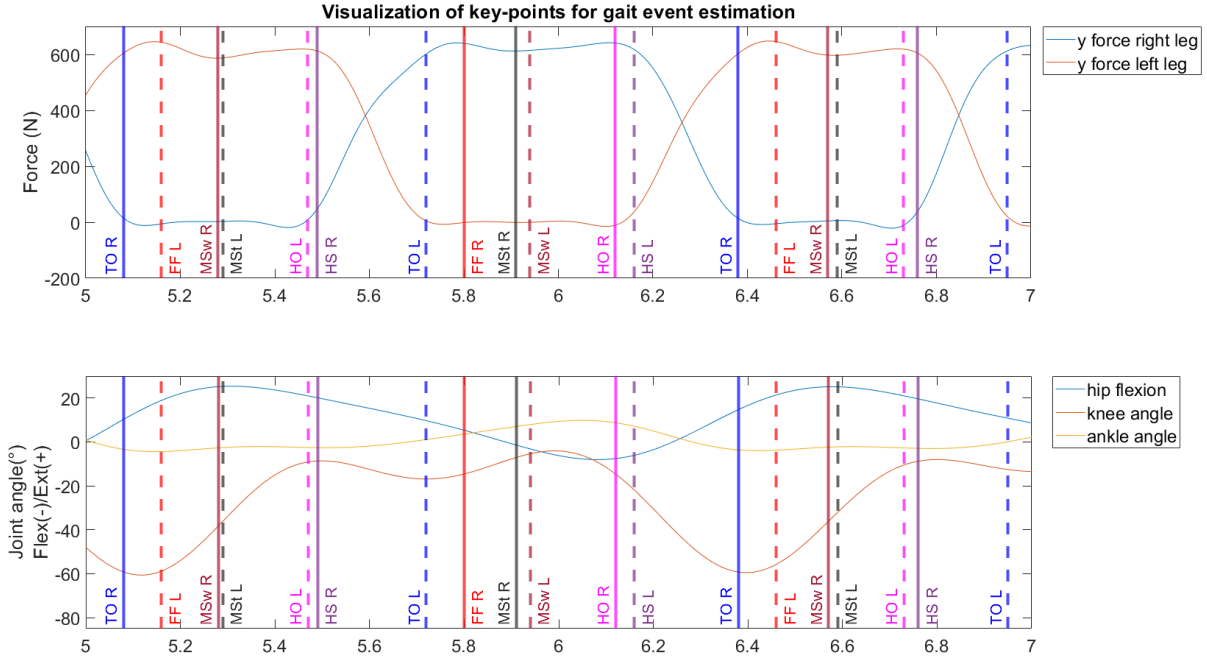

Figure 4: Comparison of reference gait events to joint angles. With GRF data in the upper figure and joint angles in the lower figure. Inserted lines indicate gait event time points from the GRF reference data of subject three at 2.7 km/h. The lines from GRF are also plotted in the joint angle data. The solid lines and dotted lines depict the gait events of, respectively, the right and left leg. The TO, MSw, HS, FF, MSt and HO are shown in the colors blue, brown, purple, red, black and pink, respectively

4.3 ASSESSMENT OF GAIT EVENT DETECTION

4.3.1 *Gait event detection in healthy subjects*

The data of gait event detection comparison for each subject can be found in tables 6 to 8. The data for the lowest walking speed of 0.9 km/h was omitted, due to the extreme offsets and RMSE values. This is also noticeable in the 1.8 km/h walking speed, having the lowest overall accuracy. This is reflected in both the offset and the RMSE which are above 100ms for most gait events. At walking speeds of 2.7 and 3.6 km/h, accuracy improved, showcased by the lower offset and RMSE. The data for each gate event was averaged for all three subjects to obtain more precise data for the detection accuracy of each gait event. All average data can be found in table 3, while tables 9 to 20 show the average and individual subject data for single gait events.

The algorithm often identifies the predicted gait events before the reference gait event at 1.8 km/h, both before and after the reference at 2.7 km/h and often after the reference at 3.6 km/h. This indicates a trend where the time points of the key points increase when gait velocity increases. The data of 1.8 km/h walking speed has a very low accuracy compared to the other two walking speeds. This is reflected in both the offset and RMSE values that are above

100ms for most gait events. With the RMSE depicting the best method to validate accuracy. When looking at the data at 2.7 km/h and 3.6 km/h, it is noticeable that most gait events have much better accuracy at one of the walking speeds compared to the other. When looking at the gait events of the right HS, TO and MSw, and the left HS, HO, and MSw it can be seen that the data at 2.7 km/h have an RMSE and Offset that is lower than those at 3.6 km/h.

Table 3: Average gait events of all healthy subjects at three different walking speeds of 1.8, 2.7 and 3.6 km/h for all discussed gait events of both legs. Data for both offsets as the RMSE is shown in milliseconds. The offset was obtained by averaging the difference between the reference key points and predicted key points in time, with the standard deviation showing variability between the gait cycles. Lastly, the RMSE shows the average difference between the predicted and the reference key points in time

Gait event	**v=1.8 km/h**		**v=2.7 km/h**		**v=3.6 km/h**	
	Offset (ms)	RMSE (ms)	Offset (ms)	RMSE (ms)	Offset (ms)	RMSE (ms)
HS R	91±50	131±89	-2±31	43±14	-79±20	82±9
FF R	253±74	283±118	83±32	116±81	-3±20	55±17
MSt R	42±55	82±31	-1±35	42±19	-40±24	50±21
HO R	29±37	54±8	42±24	52±9	3±17	21±7
TO R	89±46	107±38	-16±27	36±16	-94±12	96±15
MSw R	134±37	149±64	16±23	38±8	-78±16	81±16
HS L	118±31	124±29	59±40	71±18	-5±38	38±26
FF L	155±39	163±39	65±28	73±23	-28±35	46±15
MSt L	119±55	135±36	43±36	57±10	-36±34	51±20
HO L	24±64	107±48	-14±36	47±13	-74±20	76±9
TO L	186±69	226±123	4±30	72±34	-72±18	77±27
MSw L	63±47	98±54	-26±23	44±21	-91±20	93±10

4.3.2 *Gait event detection in stroke subjects*

The knee showcased an extension higher than 0°, however, OpenSim does not simulate the knee joint above 0° which caused multiple key points to show constant false negatives and false positives. The only key points that were consistent and usable were the maximum and minimum angles of the hip flexion and the maximum flexion of the knee, corresponding to the right HS, HO and FF, and the left HS HO and TO gait events. The ground reaction forces showed quite a few aberrations, with dissimilar force peaks. In addition, at certain gait cycles, there was a large noise artifact right before the measured data, which caused the need for more manual acquisition of reference data. In addition, the GRF of stroke subject 1 only had GRF data for the left leg, leaving the right leg with no reference, and thus no usable reference for this subject.

In tables 4 and 5, the gait event detection data can be found for the stroke subjects. The data shows an increase in accuracy at the fast speed in nearly all gait events, the left HO of subject 2 being an exemption. This means a more streamlined gait detection at higher walking speeds when utilizing the proposed strategy. However, the acquired Offset and RMSE values are still high in all but two gait events (right FF and left TO), showcasing an overall low accuracy with the algorithm when utilized with patients that have a walking impairment. The algorithm consistently identifies the predicted gait events of the left HS and right HO before the reference points, while all other gait events, except for right FF, are consistently identified after the reference point.

Table 4: Gait events of stroke subject 1 at two different walking speeds of 1.8 and 3.6 km/h the HS, HO and TO of the left leg. Data from both offset and RMSE is shown in milliseconds.

Gait event	**pref**		**fast**	
	Offset (ms)	RMSE(ms)	Offset(ms)	RMSE (ms)
HS L	-122±58	134	-67±50	82
HO L	149±52	157	104±63	120
TO L	39±48	61	37±44	56

Table 5: Gait events of stroke subject 2 at two different walking speeds of 1.8 and 3.6 km/h for the HS, FF and HO gait events on the right leg, and the HS, HO and TO of the left leg. Data from both offset and RMSE is shown in milliseconds.

Gait event	**pref**		**fast**	
	Offset (ms)	RMSE (ms)	Offset (ms)	RMSE (ms)
HS R	269±97	284	42±72	79
FF R	208±235	301	-19±23	28
HO R	-175±148	222	-63±128	134
HS L	-309±182	352	-197±115	224
HO L	60±59	81	58±71	88
TO L	87±32	92	20±19	27

DISCUSSION, LIMITATIONS & RECOMMENDATIONS

This thesis aimed to establish a IMU-based methodology for gait phase detection by utilizing key points in joint angles. that can be used on both healthy and post-stroke subjects, utilizing extracted joint angles to detect gait events. In addition, the methodology tried to perform gait phase detection of both legs with the data of only one leg. The results showed that for healthy subjects at lower speeds of 0.9 and 1.8 km/h, the methodology did not perform precise and accurate enough time points to be valid. At speeds 2.7 and 3.6 km/h, the methodology showed better results, with offset and RMSE that was often lower than 60 ms. For post-stroke subjects, the methodology did not perform up to standards for both walking speeds, due to high offset and RMSE. The faster walking speed did perform better than the preferred walking speed. These results show that the main aim of the thesis has been partially achieved, the methodology can be utilized to perform limited gait phase detection on healthy subjects but is severely limited in its detection and accuracy when utilized on post-stroke subjects. The additional aim of performing gait estimation for the non-recorded leg was fully achieved. While the utilized strategy to accomplish this was very rudimentary, the results showed that the gait estimation performed decently, with average RMSE values between 38 and 93 ms. Overall it has higher offset and RMSE values than the recorded right leg.

IMU-based strategies that utilized accelerometer data achieved offsets between 11 and 34 ms for the HS and TO gait events[29, 30]. When comparing those offsets with the ones in tables 6 to 8, it is noticeable that the range of offset error is large for lower walking speed at 1.8 km/h for healthy subjects and the preferred walking speed in post-stroke subjects. The results show offsets and RMSE that are too high for the data to be valid in a clinical setting. Mainly due to the lower walking speed increasing stance time and variability of gait event timing. The low accuracy signified that the proposed strategy is not utilizable for lower walking speeds. Higher walking speeds of 2.7 and 3.6 km/h showed more promising results, especially the data at 2.7 km/h. Where both the offset and RMSE are often lower than 60 ms. Subjects 2 and 3 show the best results in terms of accuracy. However, due to a small sample size of subjects, it is hard to draw complete conclusions on the overall accuracy of the used strategy. Seeing as the results between all healthy subjects are varied in terms of accuracy for certain gait events. For example in the left TO at 2.7 km/h, for which the offsets of all subjects are 93 ± 36, -19 ± 28 and -62 $\pm$ 24 ms.

From the results of the stroke subjects in tables 4 and 5 it is clear that subjects walking at a comfortable speed do not give valid results. When the subjects walked at their fastest possible speed, accuracy improved, but the data still consisted of high offsets. At this speed, the combined key point of the right FF and left TO gait events gave acceptable results in subject 2. Nearly all stroke subject data for gait event detection results were not accurate enough to be considered valid.

Lower overall accuracy was already expected for the left leg in healthy subjects, due to combining gait event detection for the right leg with gait events on the left leg. When looking at table 2, key points to identify gait events for the right leg are combined with gait events on the left leg, based on contra-lateral movement during walking. The data in tables 6 to 8, showed

that gait event estimation of the left leg is less accurate than the gait event detection of the right leg at 2.7 km/h for healthy subjects, with the left FF gait event being an extreme outlier for subject 1. In stroke subjects, it was expected that the left leg would have a lower accuracy, due to it being the impaired leg of the subject. Thus altering joint angles and influencing the results from chosen key points. However, this could not be evaluated due to missing reference GRF data and knee angle data that was capped at 0° by the utilized modeling software, limiting the number of key points that could be evaluated for post-stroke subjects.

Another influence on accuracy could have been due to the varying accuracy of IMU IK. During the acquisition of joint angles, certain data sets or models had rotations in the y or z directions, potentially influencing the accuracy of the obtained joint angles. In addition, for the stroke subjects, all data sets had the knee limited to 0° by OpenSim when extending, sometimes creating an angle of 0° for more than half of the stance phase. This caused the key points of the knee angle at the two full extensions and the small flexion wave in between to be unusable, severely limiting the proposed gait phase detection method. The inconsistencies during IMU IK could be attributed to the tendency of the IMU-measured angular rate to be affected by noise signal and sensor bias. Seen as the orientation is usually acquired by integration of the angular rate[31]. The noise caused by the integration of the angular rate was one of the reasons why ankle angles were not utilized. The angular velocity is lower in the ankle joint during the gait cycle compared to the hip and knee joint, causing an inferior signal-noise ratio These inconsistencies could also be caused by sub-optimal calibration measurements, shifting of IMUs during movement, or a wrongly chosen IMU heading.

The inconsistencies during IMU IK in combination with the factor of each subject having a different gait or an impaired gait created a high possibility of lower accuracy in the data. Especially with lower speeds, where joint angles showed large standard deviation, as seen in fig. 3. This limited the thesis to mainly show that a setup consisting of four IMUs, can provide rudimentary gait event detection at certain speeds in healthy subjects. In addition, gait event detection was severely limited when applying the strategy to post-stroke subjects. The limited usage was mainly due to the inability of the algorithm to filter out all the inconsistent joint angle trajectories and the artifacts in reference GRF data. Results were also limited due to the knee angle data that was capped at 0° by the utilized modeling software, limiting the number of key points that could be evaluated for post-stroke subjects.

Firstly for further recommendations, an increase of sample size would give a more validated overview of the accuracy. Secondly, possibly looking into an algorithm based on height, sex, or basic gait parameters to calculate angles at which certain gait events happen. For example, shortly after the knee reaches full flexion, at a flexion of around 40-50°, the opposite leg will be in a flat foot position.[12] This way the FF could potentially become more accurate. The left and right FF at walking speeds of 1.8 and 2.7 km/h in tables 6 to 8, are the values that have the largest inaccuracy. Furthermore, To create more potential key points to identify gait events, the angular velocity of the foot could be integrated into the algorithm. This could lead to more accurate values of the HS, FF, HO and potentially TO on the right leg for healthy subjects and left leg for stroke subjects, as done in the research of Soliman et al.[11]. HS and HO events could also be detected by utilizing data from pressure insoles as done in Donahue et al.[32]. Lastly, a methodology utilizing a more advanced algorithm such as an extended Kalman filter can be incorporated to obtain the gait events. The study of Lora-Millan et al.[12] already showed that this setup can achieve accurate gait phase detection.

CONCLUSION

As said in chapter 1, this thesis aimed to establish a IMU-based methodology for gait phase detection by utilizing key points in joint angles. Additional aims were to see if the methodology could be used on data from post-stroke subjects and to see if gait phase estimation of the non-recorded contralateral leg is possible with the data of the recorded leg.

Results in table 3 showed that the methodology does have the potential to accomplish the main aim. The gait phase detection was not accurate enough to replace the gold standard in a clinical setting. However, the data from healthy subjects did show that the gait events can be detected with an algorithm that utilizes key points in joint angles retrieved by IMUs. The second aim of the thesis could not be determined with the utilized algorithm and subject data. The algorithm did not achieve accurate full gait event detection for the post-stroke subjects with current data, showcased by the missing gait events and high RMSE values. The third aim was partially achieved, as seen from results in table 3 and tables 4 and 5. These showed that, while the gait events from the leg with recorded data were overall more accurate than those of the contralateral leg, the gait events of the contralateral leg could somewhat be estimated.

With the findings of this thesis, it can be concluded that the algorithm based on identifying key points in joint angles retrieved by IMUs has the potential to be utilized for gait phase detection. If the used algorithm can be optimized or expanded further upon with more refined processing techniques, accuracy could be improved to the standard needed for clinical usage.

If the golden standard for gait phase detection can be replaced by an IMU-based strategy, data recordings can be made outside of the lab-constrained environments. First of all causing a considerable reduction in costs, intrusiveness and set-up time. Secondly, widening the range of recordable environments, especially in terms of long-term real-world activities that show more realistic gait patterns. This could provide athletes, researchers and clinicians with a higher quantity and wider range of data.

BIBLIOGRAPHY

[1] Wenqi Liang, Fanjie Wang, Ao Fan, Wenrui Zhao, Wei Yao, and Pengfei Yang. 'Extended Application of Inertial Measurement Units in Biomechanics: From Activity Recognition to Force Estimation.' In: *Sensors* 23.9 (2023). ISSN: 1424-8220. DOI: 10.3390/s23094229. URL: https://www.mdpi.com/1424-8220/23/9/4229.

[2] A Salarian, H Russmann, F J G Vingerhoets, C Dehollain, Y Blanc, P R Burkhard, and K Aminian. 'Gait assessment in Parkinson's disease: toward an ambulatory system for long-term monitoring.' In: *IEEE Transactions on Biomedical Engineering* 51.8 (2004), pp. 1434–1443. DOI: 10.1109/TBME.2004.827933.

[3] Zhengwei Fei and Chuanjie Zhao. 'Evaluation Algorithm of Fencing Athletes' Strength Distribution Characteristics Based on Gait Tracking.' In: *Mobile Information Systems* 2022 (2022). Ed. by Mian Ahmad Jan, p. 3602776. ISSN: 1574-017X. DOI: 10.1155/2022/3602776. URL: https://doi.org/10.1155/2022/3602776.

[4] Ivana Kiprijanovska, Hristijan Gjoreski, and Matjaž Gams. 'Detection of Gait Abnormalities for Fall Risk Assessment Using Wrist-Worn Inertial Sensors and Deep Learning.' In: *Sensors* 20.18 (2020). ISSN: 1424-8220. DOI: 10.3390/s20185373. URL: https://www.mdpi.com/1424-8220/20/18/5373.

[5] Alvaro Muro-de-la Herran, Begonya Garcia-Zapirain, and Amaia Mendez-Zorrilla. 'Gait analysis methods: an overview of wearable and non-wearable systems, highlighting clinical applications.' eng. In: *Sensors (Basel, Switzerland)* 14.2 (Feb. 2014), pp. 3362–3394. ISSN: 1424-8220 (Electronic). DOI: 10.3390/s140203362.

[6] Shirley Handelzalts, Itshak Melzer, and Nachum Soroker. 'Analysis of Brain Lesion Impact on Balance and Gait Following Stroke.' In: *Frontiers in Human Neuroscience* 13 (May 2019). ISSN: 1662-5161. DOI: 10.3389/fnhum.2019.00149. URL: https://www.frontiersin.org/article/10.3389/fnhum.2019.00149/full.

[7] Carmen Ridao-Fernández, Elena Pinero-Pinto, and Gema Chamorro-Moriana. 'Observational Gait Assessment Scales in Patients with Walking Disorders: Systematic Review.' In: *BioMed Research International* 2019 (Oct. 2019), pp. 1–12. ISSN: 2314-6133. DOI: 10.1155/2019/2085039. URL: https://www.hindawi.com/journals/bmri/2019/2085039/.

[8] B. Toro, C. Nester, and P. Farren. 'A review of observational gait assessment in clinical practice.' In: *Physiotherapy Theory and Practice* 19.3 (Jan. 2003), pp. 137–149. ISSN: 0959-3985. DOI: 10.1080/09593980307964. URL: http://www.tandfonline.com/doi/full/10.1080/09593980307964.

[9] Yan Zhang, Meizi Wang, Jan Awrejcewicz, Gusztáv Fekete, Feng Ren, and Yaodong Gu. 'Using Gold-standard Gait Analysis Methods to Assess Experience Effects on Lower-limb Mechanics During Moderate High-heeled Jogging and Running.' eng. In: *Journal of visualized experiments : JoVE* 127 (Sept. 2017). ISSN: 1940-087X (Electronic). DOI: 10.3791/55714.

[10] A Peruzzi, U Della Croce, and A Cereatti. 'Estimation of stride length in level walking using an inertial measurement unit attached to the foot: a validation of the zero velocity assumption during stance.' eng. In: *Journal of biomechanics* 44.10 (July 2011), pp. 1991–1994. ISSN: 1873-2380 (Electronic). DOI: 10.1016/j.jbiomech.2011.04.035.

[11] Ahmed Soliman, Guilherme A Ribeiro, Andres Torres, Li-Fan Wu, and Mo Rastgaar. 'Gait Phase Estimation of Unsupervised Outdoors Walking Using IMUs and a Linear Regression Model.' In: *IEEE Access* 10 (2022), pp. 128090–128100. DOI: 10.1109/ACCESS.2022.3227344.

[12] Julio S Lora-Millan, Andres F Hidalgo, and Eduardo Rocon. 'An IMUs-Based Extended Kalman Filter to Estimate Gait Lower Limb Sagittal Kinematics for the Control of Wearable Robotic Devices.' In: *IEEE Access* 9 (2021), pp. 144540–144554. DOI: 10.1109/ACCESS.2021.3122160.

[13] Physiopedia. *Gait*. 2015. URL: https://www.physio-pedia.com/Gait.

[14] Roberto Grujičić. *Gait cycle*. 2023. URL: https://www.kenhub.com/en/library/anatomy/gait-cycle.

[15] Physiopedia. *Instrumented Gait Analysis*. 2022. URL: https://www.physio-pedia.com/Instrumented_Gait_Analysis.

[16] Aboelmagd Noureldin, Tashfeen B. Karamat, and Jacques Georgy. *Fundamentals of Inertial Navigation, Satellite-based Positioning and their Integration*. Berlin, Heidelberg: Springer Berlin Heidelberg, 2013. ISBN: 978-3-642-30465-1. DOI: 10.1007/978-3-642-30466-8. URL: https://link.springer.com/10.1007/978-3-642-30466-8.

[17] Christopher Jekeli. *Inertial Navigation Systems with Geodetic Applications*. Berlin, Boston: De Gruyter, 2001. ISBN: 9783110800234. DOI: doi:10.1515/9783110800234. URL: https://doi.org/10.1515/9783110800234.

[18] Mustafa Sarshar, Sasanka Polturi, and Lutz Schega. 'Gait Phase Estimation by Using LSTM in IMU-Based Gait Analysis—Proof of Concept.' In: *Sensors* 21.17 (2021). ISSN: 1424-8220. DOI: 10.3390/s21175749. URL: https://www.mdpi.com/1424-8220/21/17/5749.

[19] Sangheon Park and Sukhoon Yoon. 'Validity Evaluation of an Inertial Measurement Unit (IMU) in Gait Analysis Using Statistical Parametric Mapping (SPM).' In: *Sensors* 21.11 (2021). ISSN: 1424-8220. DOI: 10.3390/s21113667. URL: https://www.mdpi.com/1424-8220/21/11/3667.

[20] Andrés F Hidalgo, Julio S Lora-Millán, and Eduardo Rocon. 'IMU-Based Knee Angle Estimation using an Extended Kalman Filter.' In: *2019 41st Annual International Conference of the IEEE Engineering in Medicine and Biology Society (EMBC)*. 2019, pp. 570–573. DOI: 10.1109/EMBC.2019.8857614.

[21] Scott L Delp, Frank C Anderson, Allison S Arnold, Peter Loan, Ayman Habib, Chand T John, Eran Guendelman, and Darryl G Thelen. 'OpenSim: Open-Source Software to Create and Analyze Dynamic Simulations of Movement.' In: *IEEE Transactions on Biomedical Engineering* 54.11 (2007), pp. 1940–1950. DOI: 10.1109/TBME.2007.901024.

[22] Ajay Seth et al. 'OpenSim: Simulating musculoskeletal dynamics and neuromuscular control to study human and animal movement.' In: *PLOS Computational Biology* 14.7 (2018), pp. 1–20. DOI: 10.1371/journal.pcbi.1006223. URL: https://doi.org/10.1371/journal.pcbi.1006223.

[23] Ajay Seth et al. *How Scaling Works - OpenSim Documentation*. URL: https://simtk-confluence.stanford.edu:8443/display/OpenSim/How+Scaling+Works.

[24] Ajay Seth et al. *How IMU Inverse Kinematics Works - OpenSim Documentation*. URL: https://simtk-confluence.stanford.edu:8443/display/OpenSim/How+IMU+Inverse+Kinematics+Works.

[25] Huawei Wang, Akash Basu, Guillaume Durandau, and Massimo Sartori. 'A wearable real-time kinetic measurement sensor setup for human locomotion.' In: *Wearable Technologies* 4 (2023), e11. DOI: 10.1017/wtc.2023.7.

[26] Donatella Simonetti, Maartje Hendriks, Joost Herijgers, Carmen Cuerdo del Rio, Bart Koopman, Noel Keijsers, and Massimo Sartori. 'Automated spatial localization of ankle muscle sites and model-based estimation of joint torque post-stroke via a wearable sensorised leg garment.' In: *Journal of Electromyography and Kinesiology* 72 (2023), p. 102808. ISSN: 1050-6411. DOI: https://doi.org/10.1016/j.jelekin.2023.102808. URL: https://www.sciencedirect.com/science/article/pii/S1050641123000676.

[27] Kasbparast Mehdi. 'Assessment of the Muscle Strength and Range of Motion Ankle in Boys With and Without Flatfoot.' In: *Research & Investigations in Sports Medicine* 1.2 (Nov. 2017). ISSN: 25771914. DOI: 10.31031/RISM.2017.01.000509. URL: http://crimsonpublishers.com/rism/fulltext/RISM.000509.php.

[28] Yonatan C A Hutabarat, Waree Kongprawechnon, and Kittipong Ekkachai. 'Rule Based Intent Recognizer in Sit to Stand Movement Based on Knee Angle and Ground Reaction Force.' In: *2017 5th International Conference on Instrumentation, Communications, Information Technology, and Biomedical Engineering (ICICI-BME)*. IEEE, Nov. 2017, pp. 147–151. ISBN: 978-1-5386-3455-4. DOI: 10.1109/ICICI-BME.2017.8537767. URL: https://ieeexplore.ieee.org/document/8537767/.

[29] Jan M Jasiewicz, John H J Allum, James W Middleton, Andrew Barriskill, Peter Condie, Brendan Purcell, and Raymond Che Tin Li. 'Gait event detection using linear accelerometers or angular velocity transducers in able-bodied and spinal-cord injured individuals.' In: *Gait & Posture* 24.4 (2006), pp. 502–509. ISSN: 0966-6362. DOI: https://doi.org/10.1016/j.gaitpost.2005.12.017. URL: https://www.sciencedirect.com/science/article/pii/S0966636206000129.

[30] R W Selles, M A G Formanoy, J B J Bussmann, P J Janssens, and H J Stam. 'Automated estimation of initial and terminal contact timing using accelerometers; development and validation in transtibial amputees and controls.' In: *IEEE Transactions on Neural Systems and Rehabilitation Engineering* 13.1 (2005), pp. 81–88. DOI: 10.1109/TNSRE.2004.843176.

[31] Zhelong Wang and Ran Ji. 'Estimate spatial-temporal parameters of human gait using inertial sensors.' In: *2015 IEEE International Conference on Cyber Technology in Automation, Control, and Intelligent Systems (CYBER)*. 2015, pp. 1883–1888. DOI: 10.1109/CYBER.2015.7288234.

[32] Seth R Donahue and Michael E Hahn. 'Validation of Running Gait Event Detection Algorithms in a Semi-Uncontrolled Environment.' eng. In: *Sensors (Basel, Switzerland)* 22.9 (Apr. 2022). ISSN: 1424-8220 (Electronic). DOI: 10.3390/s22093452.

A

APPENDIX

Table 6: Gait events of subject 1 at three different walking speeds of 1.8, 2.7 and 3.6 km/h.

Gait event	**v=1.8km/h**		**v=2.7km/h**		**v=3.6km/h**	
	Offset (ms)	RMSE (ms)	Offset (ms)	RMSE (ms)	Offset (ms)	RMSE (ms)
HS R	206±53	212	40±39	56	-89±21	91
FF R	397±56	401	183±36	186	67±27	72
MSt R	88±69	110	5±19	19	-23±17	29
HO R	59±21	63	52±21	56	15±16	22
TO R	136±48	144	-2±33	32	-94±6	95
MSw R	201±42	205	38±26	46	-69±16	71
HS L	127±30	130	71±27	76	-1±14	14
FF L	199±46	204	87±38	94	-21±47	51
MSt L	167±50	174	53±40	66	-41±45	60
HO L	141±64	154	23±44	49	-80±18	82
TO L	340±53	344	93±36	100	-40±12	42
MSw L	113±64	129	-17±17	24	-90±9	90

Table 7: Gait events of subject 2 at three different walking speeds of 1.8, 2.7 and 3.6 km/h.

Gait event	**v=1.8km/h**		**v=2.7km/h**		**v=3.6km/h**	
	Offset (ms)	RMSE (ms)	Offset (ms)	RMSE (ms)	Offset (ms)	RMSE (ms)
HS R	29±48	56	-26±31	40	-77±21	80
FF R	202±76	215	64±30	70	-30±24	39
MSt R	-21±45	48	-28±49	56	-65±25	70
HO R	-7±51	50	23±35	41	-14±23	27
TO R	43±55	69	-41±28	50	-109±17	111
MSw R	68±40	78	-20±26	32	-97±20	99
HS L	84±32	90	44±23	49	-5±19	19
FF L	125±39	131	42±23	48	-44±32	55
MSt L	81±75	109	25±40	47	-49±34	60
HO L	-53±63	81	-41±40	57	-77±23	80
TO L	125±67	141	-19±28	33	-90±17	91
MSw L	-21±16	26	-62±15	64	-103±12	104

Table 8: Gait events of subject 3 at three different walking speeds of 1.8, 2.7 and 3.6 km/h.

Gait event S6	**v=1.8km/h**		**v=2.7km/h**		**v=3.6km/h**	
	Offset (ms)	RMSE (ms)	Offset (ms)	RMSE (ms)	Offset (ms)	RMSE (ms)
HS R	39±50	61	-21±19	28	-72±17	74
FF R	161±87	181	3±30	30	-46±19	50
MSt R	59±48	75	21±37	42	-33±28	43
HO R	35±34	48	51±6	57	9±10	13
TO R	89±32	94	-5±17	18	-80±11	81
MSw R	134±28	137	30±16	34	-69±11	70
HS L	142±31	146	61±59	84	-9±62	62
FF L	140±29	143	66±20	69	-20±19	27
MSt L	108±31	113	51±27	57	-17±19	25
HO L	-16±64	63	-23±21	31	-64±18	66
TO L	92±84	122	-62±24	66	-85±23	88
MSw L	96±48	106	2±33	32	-79±32	85

Table 9: Offset and RMSE values of right HS gait event for all subjects at three different walking speeds of 1.8, 2.7 and 3.6 km/h.

HS R Subject	**v=1.8km/h**		**v=2.7km/h**		**v=3.6km/h**	
	Offset (ms)	RMSE (ms)	Offset (ms)	RMSE (ms)	Offset (ms)	RMSE (ms)
1	206±53	212	40±39	56	-89±21	91
2	29±48	56	-26±31	40	-77±21	80
3	39±50	61	-21±19	28	-72±17	74
Average	91±50	131±89	-2±31	43±14	-79±20	82±9

Table 10: Offset and RMSE values of right FF gait event for all subjects at three different walking speeds of 1.8, 2.7 and 3.6 km/h.

FF R Subject	**v=1.8km/h**		**v=2.7km/h**		**v=3.6km/h**	
	Offset (ms)	RMSE (ms)	Offset (ms)	RMSE (ms)	Offset (ms)	RMSE (ms)
1	397±56	401	183±36	186	67±27	72
2	202±76	215	64±30	70	-30±24	39
3	161±87	181	3±30	30	-46±19	50
Average	253±74	283±118	83±32	116±81	-3±20	55±17

Table 11: Offset and RMSE values of right MSt gait event for all subjects at three different walking speeds of 1.8, 2.7 and 3.6 km/h.

MSt R Subject	**v=1.8km/h**		**v=2.7km/h**		**v=3.6km/h**	
	Offset (ms)	RMSE (ms)	Offset (ms)	RMSE (ms)	Offset (ms)	RMSE (ms)
1	88±69	110	5±19	19	-23±17	29
2	-21±45	48	-28±49	56	-65±25	70
3	59±48	75	21±37	42	-33±28	43
Average	42±55	82±31	-1±35	42±19	-40±24	50±21

Table 12: Offset and RMSE values of right HO gait event for all subjects at three different walking speeds of 1.8, 2.7 and 3.6 km/h.

HO R Subject	**v=1.8km/h**		**v=2.7km/h**		**v=3.6km/h**	
	Offset (ms)	RMSE (ms)	Offset (ms)	RMSE (ms)	Offset (ms)	RMSE (ms)
1	59±21	63	52±21	56	15±16	22
2	-7±51	50	23±35	41	-14±23	27
3	35±34	48	51±6	57	9±10	13
Average	29±37	54±8	42±24	52±9	3±17	21±7

Table 13: Offset and RMSE values of right TO gait event for all subjects at three different walking speeds of 1.8, 2.7 and 3.6 km/h.

TO R Subject	**v=1.8km/h**		**v=2.7km/h**		**v=3.6km/h**	
	Offset (ms)	RMSE (ms)	Offset (ms)	RMSE (ms)	Offset (ms)	RMSE (ms)
1	136±48	144	-2±33	32	-94±6	95
2	43±55	69	-41±28	50	-109±17	111
3	89±32	94	-5±17	18	-80±11	81
Average	89±46	107±38	-16±27	36±16	-94±12	96±15

Table 14: Offset and RMSE values of right MSw gait event for all subjects at three different walking speeds of 1.8, 2.7 and 3.6 km/h.

MSw R Subject	**v=1.8km/h**		**v=2.7km/h**		**v=3.6km/h**	
	Offset (ms)	RMSE (ms)	Offset (ms)	RMSE (ms)	Offset (ms)	RMSE (ms)
1	201±42	205	38±26	46	-69±16	71
2	68±40	78	-20±26	32	-97±20	99
3	134±28	137	30±16	34	-69±11	70
Average	134±37	149±64	16±23	38±8	-78±16	81±16

Table 15: Offset and RMSE values of left HS gait event for all subjects at three different walking speeds of 1.8, 2.7 and 3.6 km/h.

HS L Subject	**v=1.8km/h**		**v=2.7km/h**		**v=3.6km/h**	
	Offset (ms)	RMSE (ms)	Offset (ms)	RMSE (ms)	Offset (ms)	RMSE (ms)
1	127±30	130	71±27	76	-1±14	14
2	84±32	90	44±23	49	-5±19	19
3	142±31	146	61±59	84	-9±62	62
Average	118±31	124±29	59±40	71±18	-5±38	38±26

Table 16: Offset and RMSE values of left FF gait event for all subjects at three different walking speeds of 1.8, 2.7 and 3.6 km/h.

FF L Subject	**v=1.8km/h**		**v=2.7km/h**		**v=3.6km/h**	
	Offset (ms)	RMSE (ms)	Offset (ms)	RMSE (ms)	Offset (ms)	RMSE (ms)
1	199±46	204	87±38	94	-21±47	51
2	125±39	131	42±23	48	-44±32	55
3	140±29	143	66±20	69	-20±19	27
Average	155±39	163±39	65±28	73±23	-28±35	46±15

Table 17: Offset and RMSE values of left MSt gait event for all subjects at three different walking speeds of 1.8, 2.7 and 3.6 km/h.

MSt L Subject	**v=1.8km/h**		**v=2.7km/h**		**v=3.6km/h**	
	Offset (ms)	RMSE (ms)	Offset (ms)	RMSE (ms)	Offset (ms)	RMSE (ms)
1	167±50	174	53±40	66	-41±45	60
2	81±75	109	25±40	47	-49±34	60
3	108±31	113	51±27	57	-17±19	25
Average	119±55	135±36	43±36	57±10	-36±34	51±20

Table 18: Offset and RMSE values of left HO gait event for all subjects at three different walking speeds of 1.8, 2.7 and 3.6 km/h.

HO L Subject	**v=1.8km/h**		**v=2.7km/h**		**v=3.6km/h**	
	Offset (ms)	RMSE (ms)	Offset (ms)	RMSE (ms)	Offset (ms)	RMSE (ms)
1	141±64	154	23±44	49	-80±18	82
2	-53±63	81	-41±40	57	-77±23	80
3	-16±64	63	-23±21	31	-64±18	66
Average	24±64	107±48	-14±36	47±13	-74±20	76±9

Table 19: Offset and RMSE values of left TO gait event for all subjects at three different walking speeds of 1.8, 2.7 and 3.6 km/h.

TO L Subject	**v=1.8km/h**		**v=2.7km/h**		**v=3.6km/h**	
	Offset (ms)	RMSE (ms)	Offset (ms)	RMSE (ms)	Offset (ms)	RMSE (ms)
1	340±53	344	93±36	100	-40±12	42
2	125±67	141	-19±28	33	-90±17	91
3	92±84	122	-62±24	66	-85±23	88
Average	186±69	226±123	4±30	72±34	-72±18	77±27

Table 20: Offset and RMSE values of left MSw gait event for all subjects at three different walking speeds of 1.8, 2.7 and 3.6 km/h.

MSw L Subject	**v=1.8km/h**		**v=2.7km/h**		**v=3.6km/h**	
	Offset (ms)	RMSE (ms)	Offset (ms)	RMSE (ms)	Offset (ms)	RMSE (ms)
1	113±64	129	-17±17	24	-90±9	90
2	-21±16	26	-62±15	64	-103±12	104
3	96±48	106	2±33	32	-79±32	85
Average	63±47	98±54	-26±23	44±21	-91±20	93±10